ARTICLE

MOFs based on 1D structural sub-domains with Brønsted acid and redox active sites as effective bi-functional catalysts

Received 00th January 20xx,
Accepted 00th January 20xx

DOI: 10.1039/x0xx00000x

José María Moreno, Alexandra Velty and Urbano Díaz*

Novel family of lamellar MOF-type materials, which contain Brønsted acid sites together with redox active centers, based on assembled 1D organic-inorganic nanoribbons were obtained through direct solvothermal synthesis routes, using specific monotopic benzylcarboxylate spacers with thiol substituents in *para*-position like structural modulator compounds and effective post-synthesis oxidized treatments to generate accessible sulfonic groups. Low-dimensional aluminum metal-organic materials, containing free sulfonic pendant groups (Al-ITQ-SO_3H), were successfully tested in several acid reactions, such as acetalization, esterification and open ring of epoxides with significant impact in fine chemistry processes. The direct introduction of stabilized Pd nanoparticles, cohabitating with pendant sulfonic groups, allowed the preparation of active bi-functional MOF-type hybrid materials (Al-ITQ-SO_3H/Pd) capable to carry out one-pot two-step oxidation-acetalization reactions, exhibiting high yield and high activity during consecutive catalytic cycles.

Introduction

Hybrid porous solids are based on the bonding of structural units of different physico-chemical nature to build up 1D, 2D or 3D frameworks whose skeleton present both organic and inorganic blocks linked by stable and strong bonds. Depending on specific monomer precursors used, it is possible to obtain several types of hybrid materials such as periodic mesoporous organosilicas (PMOs), covalent organic frameworks (COFs) and metal-organic frameworks (MOFs).[1-3] Specifically, this last family are based on metal ions, metal clusters or metal-oxygen clusters as inorganic units and multitopic linkers as structural organic units.[4-5] A large number of metal-organic materials has been synthesized due to almost infinite variety of inorganic builders (based on alkaline, transition or rare earth metals) and multitopic organic spacers that it would be used and combined between them.[6] These materials present moderate chemical and thermal stability, ultra-low density and large internal surface, being ideal candidates for a wide range of applications such as catalysis, adsorption, separation, sensors, drug delivery or magnetism.[7-12]

MOFs appeared as a new opportunity in catalysis field, being presented as promising and alternative heterogeneous catalysts in many works due to their high internal porosity, allowing fast mass transport and/or interactions with substrates in which uniformity of their porous system and channel sizes are relevant to achieve high selectivity, increasing their use as effective heterogeneous catalysts in the last two decades.[13-14] Active sites into the metal-organic structures could be located in the metal nodes associated with an unsaturated coordination environment, in the catalytic species encapsulated in the internal pores and in the active inherent functions to the organic spacers.[15-20]

One of the most effective active sites present in the MOFs came from the adequate inclusion of Brønsted acid centers[21] through of incorporation of sulfonic groups, generating highly active acid metal-organic materials. Different approaches were tested to introduce sulfonic groups from post-synthetic treatments such as framework sulfonation, post-functionalization of amine groups with sultones and encapsulation of heteropolyacids. However, more direct methods such as the suitable incorporation of sulfonic groups directly during solvothermal synthesis process for MIL-101(Cr) and UiO66(Zr) were also described as effective methodologies.[22-27] Due to the presence of Brønsted acid sites in the metal-organic materials, they were tested in different reactions where high acidity was required such as esterification, Friedel-Crafts acylation, isomerization, acetalization or fructose dehydration.[28-31]

Once it is well known the high capacity of MOFs to be used as solid catalysts in heterogeneous processes, it is noteworthy to point out the possibility of step forward through of performing one-pot two-step reactions as tandem, domino or cascade reactions.[32] The fact of carrying out multiple catalytic reactions in one-pot system and using only one catalytic system presents great advantages such as reduction of waste production, energy

Instituto de Tecnología Química, Universitat Politècnica de València-Consejo Superior de Investigaciones Científicas, Avenida de los Naranjos s/n, E-46022 Valencia, Spain. E-mail: udiaz@itq.upv.es, Tel: +34963877811.

Electronic Supplementary Information (ESI) available: Characterization data related with hybrid catalysts (TEM images, TGAs and DTAs, NMR and IR spectroscopies). Additional catalytic results for the considered reactions, including leaching and recycling data. Characterization of used hybrid catalysts after reaction. See DOI: 10.1039/x0xx00000x

cost save and atom economy improve, making the catalytic processes more environmental and sustainable.[33-34] Specifically, metal-organic materials exhibit the particular advantage of containing several active sites in the same framework, obtaining multi-functional solid materials with high potential to perform one-pot consecutive catalytic processes.[35] Bi-functional metal-organic materials could be based on unsaturated metal nodes cohabitating with metal nanoparticles (NPs) or functional organic spacers, achieving good catalytic activity in different organic transformations such as oxidation-hydrogenation, de-acetalization-Henry reaction and hydrogenation-isomerization.[36-39] Different approaches to introduce NPs into the structure have been described[40] such as impregnation, wetness method, by deposition or inmobilization,[41-43] metallic NPs being located in the internal pores of the network or onto external surface.[44-45]

Considering the high relevance of this class of bi-functional metal-organic hybrid materials, a new low-dimensional family of aluminum metal-organic materials with thiol moieties were here synthesized, being these transformed in free sulfonic pendant groups by oxidation treatment and successfully tested in several acid reactions, such as acetalization, esterification and open ring of epoxides. The catalytic results demonstrated the high catalytic activity of the hybrid materials and their reusability and recyclability. Moreover, bi-functional hybrid catalysts were synthesized in one-step direct solvothermal synthesis process containing thiol pendant groups and Pd nanoparticles in the structure, the thiols moieties being converted to sulfonic groups. These bi-functional hybrid materials were capable to perform one-pot two-step oxidation-acetalization reactions, reaching high yield and exhibiting high activity during four consecutive uses. Furthermore, previously to catalytic tests, metal-organic hybrid materials were characterized by XRD, chemical analysis, TGA, NMR, IR and XPS spectroscopy, and TEM/HRTEM microscopy, being analyzed and corroborated the lamellar structure present in the framework of the hybrid materials based on the association of the 1D organic-inorganic sub-units.

Results and discussion

Synthesis and characterization

Novel metal-organic materials were synthesized through of auto-assembly of specific monotopic organic spacers with inorganic nodes, being they used as builder units to obtain new families of low-dimensional hybrid materials based in 1D organic-inorganic sub-units (Scheme 1) under specific conditions in the solvothermal synthesis process. Specifically, benzene monocarboxylate compound with thiol groups located in *para* conformation was used as organic molecular spacer (Scheme S1).

XRD patterns confirmed the lamellar structuration level achieved due to auto-assembly of the 1D nanoribbon-type units that occurred by using a mixture of two solvents with different hydrophobic-hydrophilic properties (DMF/MiliQ water), being each builder precursor totally dissolved in one of the solvents.

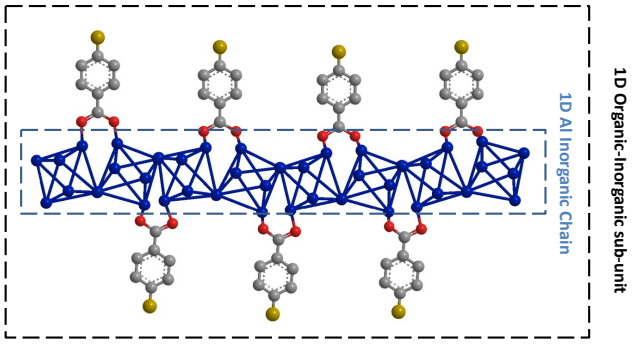

Scheme 1. 1D organic-inorganic sub-units present in the metal-organic materials.

After this, during the synthesis process, the interaction of the precursors in the generated interphases facilitated the formation of 1D organic-inorganic sub-units, which were

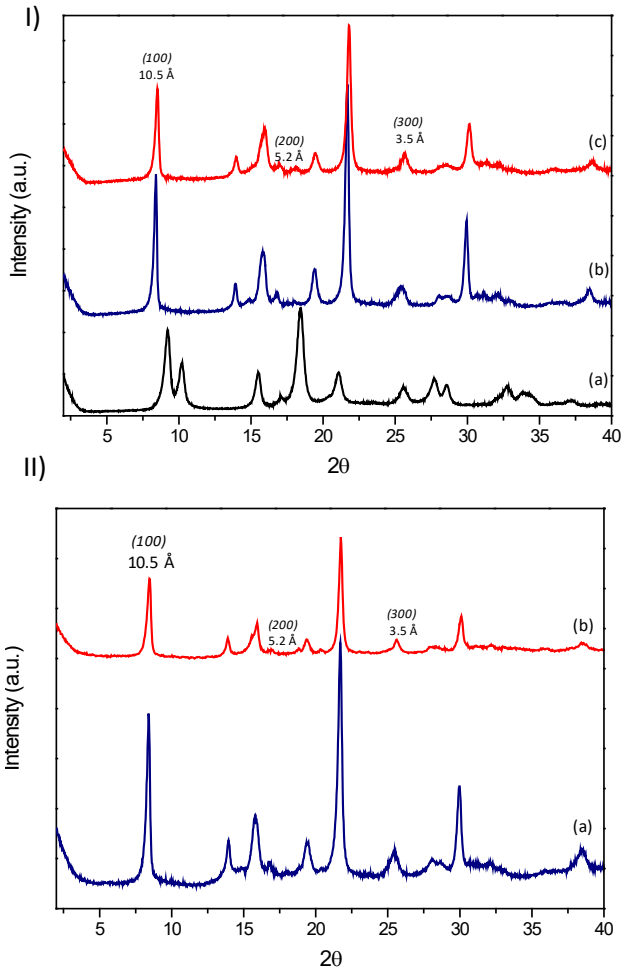

Figure 1. (I) XRD patterns of Al-metal-organic materials: (a) 3D standard MIL-53(Al), (b) Al-ITQ-SH and (c) Al-ITQ-SO_3H; (II) XRD patterns of Al-metal-organic materials: (a) Al-ITQ-SH/Pd and (c) Al-ITQ-SO_3H/Pd.

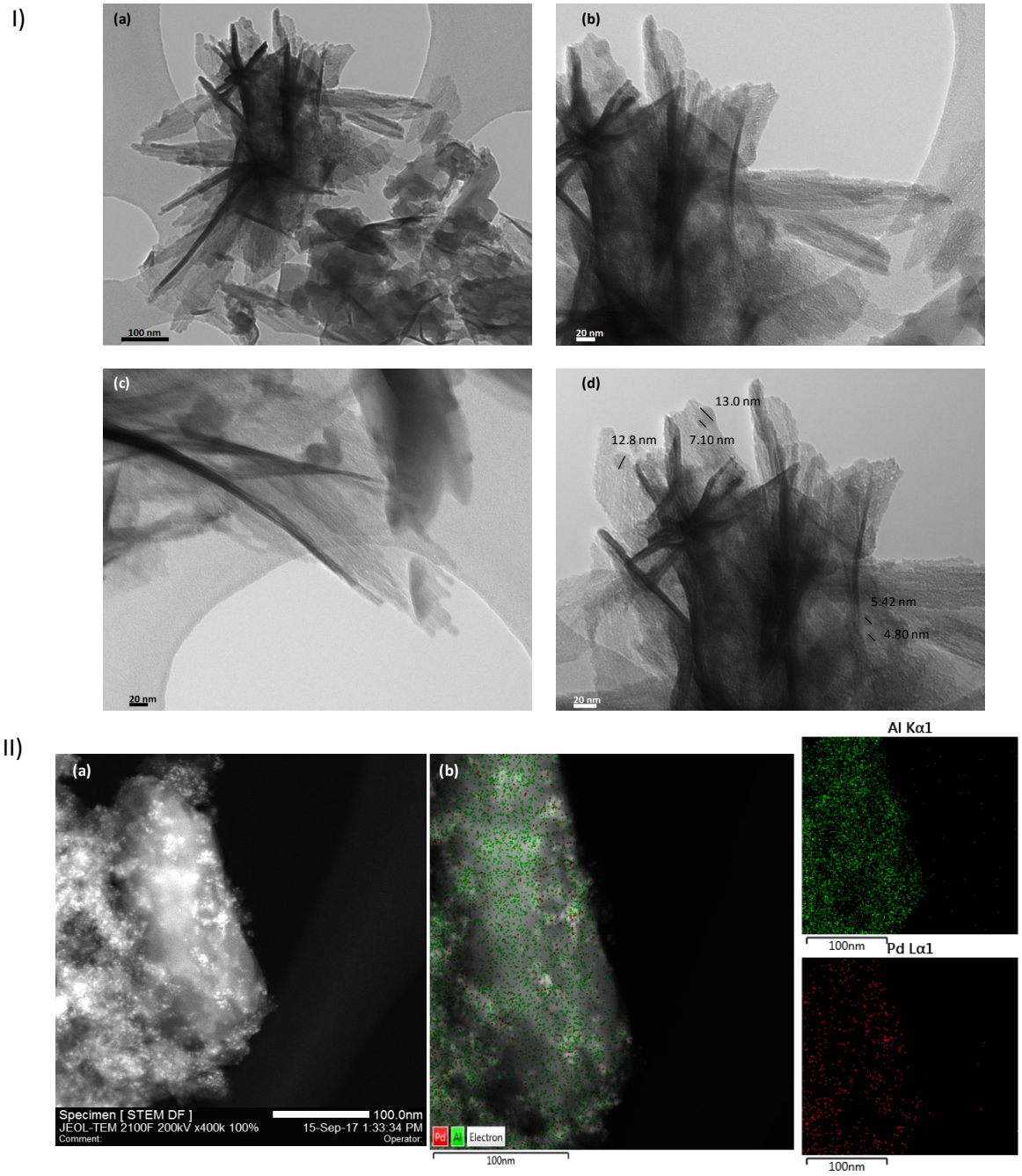

Figure 2. (I) TEM images of Al-ITQ-SH/Pd sample. Scale bars correspond to 100 nm for (a) micrograph and 20 nm for (b) (c) and (d) micrographs. (II) Al-ITQ-SO_3H/Pd sample: (a) STEM images and (b) EDS mapping of metallic elements.

associated between them at long order to produce lamellar hybrid networks. XRD diffractograms clearly revealed *(100)* low angle diffraction bands, which were characteristic of lamellar materials constituted by individual layers perpendicularly disposed to axis *a* (Figure 1 (I)). These individual sheets were probably formed for the association of 1D organic-inorganic nanoribbons where the detected basal space evidenced the separation between the individual layers due to perpendicularly location of organic spacers to aluminum inorganic nodes. In addition, from XRD diffractograms, it was possible to observe not only *(100)* diffraction band, but also further bands assigned to *(200)* and *(300)* reflections, corroborating the regular and homogeneous separation achieved between consecutive organic-inorganic sheets.

Specifically, considering the molecular length of the organic spacer containing thiol groups (-SH, ~6.0 Å), taking account that the *(100)* diffraction band was observed at ~10.5 Å and that they were probably perpendicularly located in both sides of $AlO_4(OH)_2$ chains, the thickness of each individual one-dimensional sub-unit could be calculated, being close to 4.5 Å. This value is coincident with the size of aluminum octahedra, which are forming these 1D structural domains. The obtained

Table 1. Chemical analysis of standard MIL-53(Al), Al-ITQ-SH, Al-ITQ-SO_3H, Al-ITQ-SH/Pd and Al-ITQ-SO_3H/Pd.

Samples	C[a]	H[a]	N[a]	S[a]	Org.Cont.[a]		Al[a]	Pd[a]	$C/S)_{Exp}$
					CHNS[b]	TGA[c]			
MIL-53(Al)	43.8	2.6	0	---	46.4	72.6	12.0	---	---
Al-ITQ-SH	42.6	3.7	2.1	13.6	62	77.7	10.5	---	8.3
Al-ITQ-SO_3H	35.8	3.1	0	12.8	51.7	68.3	10.6	---	7.4
Al-ITQ-SH/Pd	36.7	3.1	0.1	12.5	52.4	64.8	10.8	1.7	7.8
Al-ITQ-SO_3H/Pd	32.2	3.2	0	12.0	47.4	59.0	12.4	2.2	7.1

[a] Percentage in weight (%wt); [b] Organic content from CHNS elemental analysis, [c] Organic content from thermogravimetrical analysis without taking account hydration water.

materials were treated under oxidation conditions in order to convert the thiol moieties to sulfonic groups, being considered the obtained materials as potential Brønsted acid hybrid catalysts. After this treatment, the metal-organic materials presented practically the same XRD pattern that before oxidation process, confirming the high stability of the lamellar solids, remaining unchanged the position of *(100)* characteristic diffraction band.

Furthermore, bi-functional metal-organic materials were synthesized, achieving the same structuration level as above described (Figure 1 (II)). The main difference in this case was the effective incorporation of palladium species directly through one step synthesis. This material was based on associated 1D organic-inorganic nanoribbons, being useful the thiol groups, located perpendicularly to the aluminum nodes, to interact with the palladium precursors during the solvothermal synthesis process. This hybrid metal-organic material was treated under the same oxidation conditions, keeping the lamellar framework unchanged, being possible to observe the *(100)* diffraction before and after the oxidation treatment.

XRD results demonstrated that the solvothermal specific synthesis medium based on using two solvents with different polarities and employing monotopic organic spacers, allowed to obtain lamellar hybrid materials based on associated 1D organic-inorganic sub-units with pendant thiol groups (Scheme 1). These were easily oxidized to sulfonic groups in order to provide more active and versatile acid metal-organic materials. Moreover, palladium nanoparticles were incorporated directly in the same solvothermal one-step synthesis process, generating hybrid solids since after oxidation process a bi-functional organic-inorganic material with acid (sulfonic groups) and redox (Pd NPs) active sites in the same lamellar network was obtained (Scheme S1).

The lamellar structural level, above described for the metal-organic materials, was confirmed by electron microscopy images (TEM and HRTEM). The micrographs of Al-ITQ-SH and Al-ITQ-SO_3H materials were obtained by TEM (Figure S1), showing the formation of lamellar blocks in which it is possible to distinguish stratified crystals formed by individual layers. It is noteworthy to point out how the crystals were less agglomerated when the solid was treated under oxidation process (Figure S1 c, d). This effect could be indicative to the easy expansion phenomena, due to the elimination of the organic compounds located out of frameworks. Taking into account, the lamellar crystals were more separated, being more easily seen the stratified organization in the oxidized samples.

Furthermore, Figure 2 illustrates TEM images from Al-ITQ-SH/Pd hybrid material. First, lamellar morphology based on overlapping stratification of agglomerated layers in the material before the post-synthesis oxidation process was observed. Moreover, the size of palladium nanoparticles ranging from 5 to 13 nm was determined, being them probably located close to thiol groups which could act as stabilization agents of metallic species. The oxidized sample (Al-ITQ-SO_3H/Pd) was analyzed by TEM and HRTEM. From Figure S2 the same phenomena above described for solids without metallic species, where the materials exhibited a less agglomerated morphology was observed. Moreover, the Pd nanoparticles size was decreased and ranging from 2 to 4 nm. Specially, the order of piled individual layers based on 1D sub-units that forming this kind of metal-organic materials was clearly observed (Figure S2c). Finally, this sample was analyzed by STEM (Figure 2 (I)a) where palladium nanoparticles probably located close to thiol groups in the metal-organic structure were detected, being also identified through EDS mapping analysis (Figure 2(II)b). Intermolecular hydrogen bonding between thiol and sulfonic groups probably facilitated the stabilization and isolation of Pd nanoparticles onto the surface of the low-dimensional metalorganic architectures.[46] From EDS technique, the homogenous distribution of aluminum nodes and palladium nanoparticles, appearing more amount of aluminum due to its structural role in the hybrid network, was detected (Table 1).

The chemical analysis results of lamellar hydrid materials are summarized in Table 1. The organic content for all metal-organic materials confirmed the proper incorporation of the organic spacers into the different frameworks. Similar values for materials containing thiol groups compared with 3D standard MIL-53(Al) were found. However, the material with palladium nanoparticles showed lower organic content probably due to the introduction of palladium species that reduced the

contribution of organic spacers in the final solid. In this case, the auto-assembly of the organic and inorganic building units could be more complicated due to the presence of metallic precursors. Furthermore, the organic content in the hybrid materials containing sulfonic moieties was lower because during the oxidation post-synthesis process not only the thiol groups were oxidized, but also DMF and organic molecules occluded in the framework were removed.

After the oxidation process, the nitrogen content was almost zero, being confirmed the absence of DMF in the final hybrid materials. Taking into account the sulphur content, this was lower for the materials with palladium due to lower incorporation of the monotopic organic spacers. It is important to remark that molar ratio C/S presented values close to the theoretical (C/S=7), especially once the oxidation was completed due to release of the occluded unreacted organic compounds. Related to aluminum content, this was similar in all materials because the same structural level and topologies were achieved in all samples. Regarding palladium content, the experimental value was higher than theoretical (1%wt) because lower yield of the material and higher incorporation of palladium precursor was achieved, being even higher after the oxidation process due to elimination of the organic content located out of framework. Therefore, these results confirmed the effective incorporation of organic spacers and palladium nanoparticles in the lamellar organic-inorganic materials.

Figure S3 shows thermogravimetrical analysis (TGA) and their corresponding derivate curves (DTA) where the weight loss for the organic spacers and their hydrothermal stability was determined. In all cases, three different weight loss were found, being the first one loss due to hydration water (I). A second weight loss (II) between 150-250ºC was attributed to the residual DMF and unreacted linkers occluded in the frameworks. The third and last weight loss (III) was registered at higher temperatures (350-650ºC), being assigned to aromatic fragments from monotopic organic molecules used as spacers in the synthesis process. It is important to point out that, the contribution due to water produced by dehydration of $AlO_4(OH)_2$ builder units present in the 1D organic-inorganic sub-units was included in the analysis, explaining the higher organic content obtained from TGA compared with CHNS analysis. Additionally, the hydrothermal stability was detected from DTA curves, being clearly higher for the materials without palladium (600ºC) than when the palladium was incorporated (400-500ºC).

Spectroscopic characterization

^{13}C CP/MAS NMR spectra of Al-ITQ-SH, Al-ITQ-SO_3H, Al-ITQ-SH/Pd and Al-ITQ-SO_3H/Pd are depicted in Figure S4. The spectra corroborated the total integrity of the organic spacers in the lamellar structure of the metal-organic materials, being assigned clearly all carbon atoms to different chemical shifts. Specifically, a signal at ~170 ppm was associated to carbon atom from carboxylate group. Moreover, several signals between 110-140 ppm were detected due to carbons atoms from aromatic rings. It is important to point out that lower intensity signals were detected and attributed to the use of DMF during

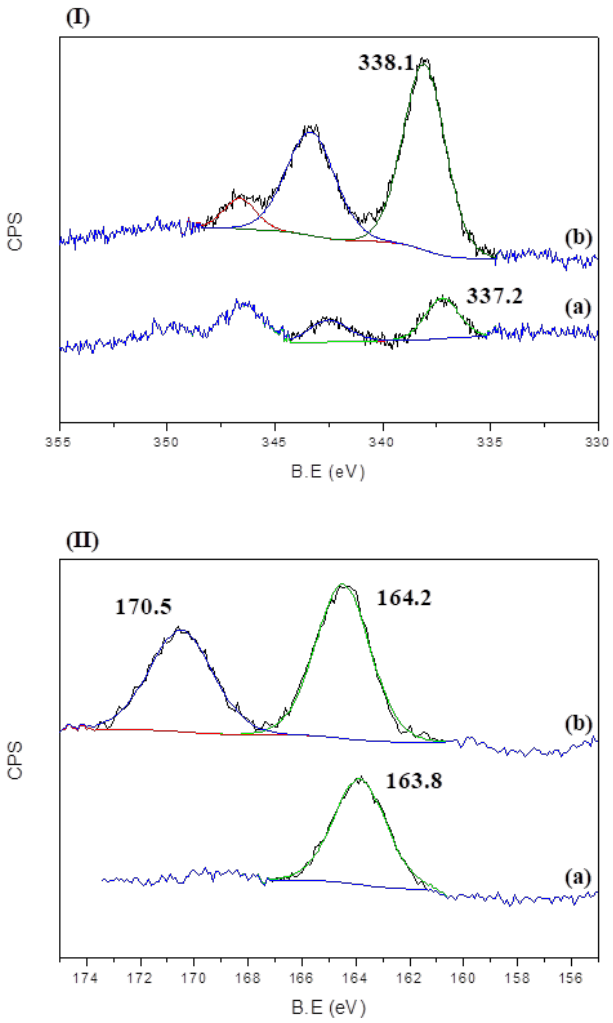

Figure 3. XPS spectra of the materials: (I) Pd3d y (II) S2p (a) Al-ITQ-SH/Pd y (b) Al-ITQ-SO_3H/Pd.

the solvothermal synthesis process for Al-ITQ-SH and also to the use of ethanol employed during the oxidation post-synthesis treatment for Al-ITQ-SO_3H samples. Additionally, a signal at ~145 ppm was assigned to sulfonic groups, being the intensity of this chemical shift lower (Figure S4b, d) because of not all thiol groups were oxidized under the post-synthesis oxidation treatment. Therefore, these results confirmed the total incorporation of the aromatic organic spacers, remaining intact as in the initial conformation, and the effectivity of post-synthesis oxidation processes of thiol groups to obtain hybrid metal-organic materials with pendant Brønsted acid sites.

In addition, ^{27}Al MAS NMR spectra of the hybrid materials are depicted in Figure S5 where the chemical environment of aluminum in the framework was analysed. Octahedral positions for the aluminum located in the inorganic chains present in the 1D organic-inorganic sub-units were identified, being specifically registered a main chemical shift at ~0 ppm. Moreover, a broad specific shoulder was observed, being due to a second quadrupole order interaction. This phenomenon was assigned to use of aqueous solvothermal synthesis medium, because of water molecules interact with aluminum

nodes promoting an electric field gradient at metallic structural nodes.

IR spectroscopy also confirmed the total integrity of organic building blocks incorporated in the framework of the hybrid materials (Figure S6). At 1400-1700 cm^{-1} range, a vibrational band assigned to the carboxylate groups from the organic spacers bond to inorganic units was observed. It is remarkably that, in this same range, several signals attributed to asymmetric stretching vibrations were detected because of aromatic rings present in the organic units. Furthermore, the spectra showed a broad signal for stretching vibration mode at 3600-3200 cm^{-1} range, coming from hydroxyl groups (-OH) due to hydration water and aluminum oxo-hydroxide species, $AlO_4(OH)_2$, present in the 1D sub-units. Therefore, IR spectroscopy also confirmed the total integrity of the organic spacers, forming the structure of the hybrid materials, being in agreement with NMR results.

XPS (X-ray Photoelectron Spectroscopy) study of the oxidation state of the palladium nanoparticles incorporated in the hybrid materials (Al-ITQ-SH/Pd and Al-ITQ-SO_3H/Pd) was performed. The spectrum of Pd3d was shown in Figure 3. Two bands were detected corresponding to components with a binding energy (B.E.) at 337.2 and 338.1 eV for Al-ITQ-SH/Pd and Al-ITQ-SO_3H/Pd, respectively. This result is typical of the presence oxidized palladium species, being not observed the metallic (Pd^0) component.[47] On the other hand, the spectrum of S2P (Figure 3(II)) confirmed the high effectiveness of the post-synthesis oxidation process due to the presence of the band with a B.E. at 163.8 eV, corresponding to the thiols groups for Al-ITQ-SH/Pd and of a new band with a higher B.E. at 170.5 eV assigned to sulfonic groups for Al-ITQ-SO_3H/Pd hybrid material.[30, 48]

Textural properties

Textural properties of aluminum metal-organic materials were characterized by argon adsorption isotherms (Figures S7 and S8). Type I isotherms were obtained for all materials, being characteristic of solids with associated microporosity. Different BET specific surfaces areas were determined for the hybrid solids, depending on the incorporation or not of the palladium nanoparticles. Specifically, Al-ITQ-SH showed a higher value (S_{BET}: 263 m^2/g) than Al-ITQ-SH/Pd (S_{BET}: 122 m^2/g), being this fact associated with the location into the pores of some palladium species, avoiding the correct diffusion of the argon molecules. Moreover, the final materials, obtained after oxidation treatments, exhibited higher values: 275 m^2/g for Al-ITQ-SO_3H and 223 m^2/g for Al-ITQ-SO_3H/Pd. This effect was probably due to elimination of the unreacted organic spacers or DMF molecules occluded in the materials, being these solids more accessible for the argon molecules (Table 2).

Moreover, Hörvath-Kawazoe pore size distribution evidenced that the majority of pores were centred around 5.5 Å for all materials (Figure S7 and S8). This low value was associated to reduced basal space due to short length of organic unit used as spacer, being typically characteristic of microporous materials with more compacted frameworks.

Finally, CO_2 adsorption isotherms (Figure S9) were measured in order to study the adsorption capacity of the aluminum hybrid materials. The results revealed difference between the different hybrid solids, being the material Al-ITQ-SH with the highest adsorption capacity, showing higher or similar adsorption values than other standard thiol and sulfonic metal-organic materials (Table S1). It is important to point out that oxidized materials presented lower adsorption values probably due to the bigger steric bulkiness of the sulfonic groups.

Table 2. Main textural properties of lamellar hybrid metal-organic materials.

Samples	S_{BET} (m^2g^{-1})	S_{micro} (m^2g^{-1})[a]	S_{ext} (m^2g^{-1})	V_{Tot} (cm^3g^{-1})	V_{micro} (cm^3g^{-1})	d_{pore} (Å)
Al-ITQ-SH	263	215	48	0.24	0.11	5.5
Al-ITQ-SO_3H	275	198	77	0.26	0.09	5.5
Al-ITQ-SH/Pd	122	53	69	0.26	0.02	5.5
Al-ITQ-SO_3H/Pd	223	170	53	0.35	0.08	5.5

[a] $S_{ext} = (S_{BET}-S_{micro})$.

Catalytic Activity

Herein we reported the synthesis of a new lamellar hybrid materials, Al-ITQ-SO_3H, based on 1D sub-units with Brønsted acid sites owing the presence of sulfonic groups. We furthermore described the preparation of bi-functional materials thanks to the incorporation of palladium nanoparticles. This new material, Al-ITQ-SO_3H/Pd, offers both Brønsted acid and redox active sites. From a catalytic point of view, this new and versatile hybrid material offers high potential in acid and redox catalysed processes. Therefore, the catalytic activity of this hybrid material has been evaluated for different type of reactions such as acetalization, esterification, ring opening and oxidation-acetalization two-step processes to provide intermediates and fine chemicals of interest in pharmaceutical, perfumery, solvents or agrochemistry industries.

Acetalization reactions

Acetalization is not only a useful tool in organic chemistry since is a reversible protection of carbonyl compounds[49] but is also widely applied to produce intermediates of reaction and compounds of interest in chemical industry such as pharmaceutical,[50] fragrance and flavours.[51] Indeed, the production of acetals can smooth down the strong smell of different carbonyl compounds.

Usually, acetalization of aldehydes with an alcohol or diol takes place in the presence of Brønsted or Lewis acids.[52-54] Several methods for the preparation of cyclic acetals were reported through of using mineral acids, resins, zeolites, mesoporous materials or metal-organic materials as catalysts for the condensation of glycols with aromatic aldehydes.[30, 55-58]

Then, to illustrate the ability of aluminum metal-organic materials with sulfonic groups (Al-ITQ-SO_3H) here synthesized as acid catalysts, we demonstrated the suitable catalytic properties deployed by the this material to produce a series of acetals with application in perfumery industry. Firstly, the

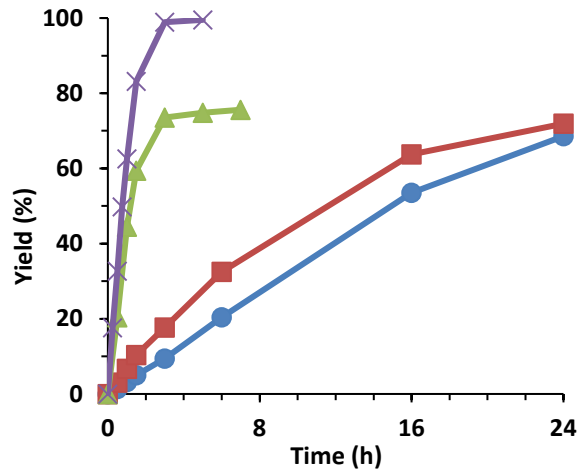

Figure 4. Kinetics of benzaldehyde propylene glycol acetal production in presence of Al-ITQ-SO_3H: (●) ratio 1:2, 10 mol% SO_3H at 90ºC, (■) ratio 1:2, 20 mol% SO_3H at 90ºC, (▲) ratio 1:6, 20 mol% SO_3H at 90ºC and (×) ratio 1:6, 20 mol% SO_3H under solvent reflux. Toluene was used as solvent. Ratio (benzaldehyde:1,2-propanediol).

acetalization of benzaldehyde with methanol was studied (Scheme 2). Benzaldehyde dimethyl acetal is commonly used as flavour and fragrance agents since it has a nutty and floral odour. The results presented in the Figure S10 confirmed that the acetalization of benzaldehyde and methanol was successfully performed in the presence of different Al-ITQ-SO_3H loading, in mild reaction conditions, at 30ºC. Moreover, only slight variations can be observed from the different kinetic curves, increasing the initial rate with the amount of active sites, giving 90 % yield with 99 % selectivity. In the same way, cyclic acetals of benzaldehyde and vanillin can be successfully prepared using propylene glycol as diol. Since acetalization is an equilibrium process, the remove of water is usually required to shift the equilibrium and achieve maximum yield and selectivity.

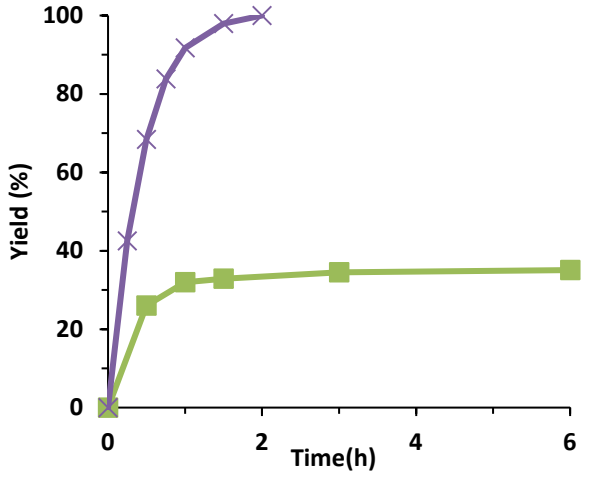

Figure 5. Yield of vanillin propylene glycol acetal versus time, when acetalization was carried out in the presence of Al-ITQ-SO_3H: (■) ratio 1:6, 20 mol% SO_3H at 90ºC and (×) ratio 1:6, 20 mol% SO_3H under solvent reflux. Toluene was used as solvent.

Both benzaldehyde and vanillin propylene glycol acetals are flavour and fragrance agents, the first due to its fruity and floral odour while the second to vanillin and sweet odour. The results presented in the Figures 4 and 5 demonstrated that, indeed, to achieve a maximum acetal yield and selectivity (99%), the azeotropic distillation of water using toluene as solvent was required. The catalytic results obtained for the synthesis of benzaldehyde propylene glycol acetal revealed that neither the increase of amount of catalyst charge nor the increase of diol/benzaldehyde mole ratio allowed to shift the thermodynamic equilibrium achieved, being the maximum yield close to 74%. The results demonstrated the adequate catalytic properties of the hybrid materials as solid acid catalysts to carry out acetalization process with methanol and diol to prepare products with high added-value in the industry of flavour and fragrance agents.

Esterification reactions

Because the acetalization process does not require strong acid sites, the catalytic activity of the sulfonic acid sites of Al-ITQ-SO_3H here synthesised was checked in strong acid catalysed reaction such as esterification. In fact, the esterification of alcohols with carboxylic acids is one of the best known and oldest chemical reactions, being based normally on a nucleophilic attack of the alcohol at the carboxylic group of the ester.[59-60] This process has extensively been studied, being published works from homogeneous catalysis by using mineral acids such as sulphuric acid to heterogeneous catalysis by using resins, zeolites, mesoporous materials, heteropolyacids or metal-organic materials as solid catalysts.[28, 61-64] Currently, there is a great interest in this reaction due to its application in different industrial applications because of organic esters are commonly used as plastic derivatives, in the solvents industry, perfumery and agrochemistry.[65]

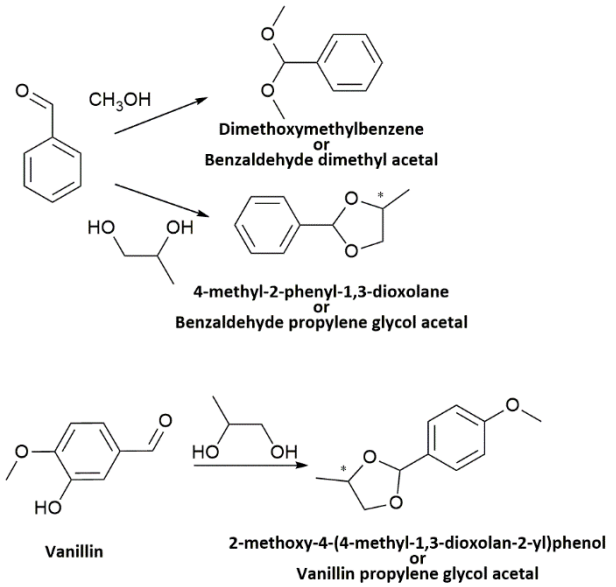

Scheme 2. Preparation of different flavor and fragrances agents by acetalization.

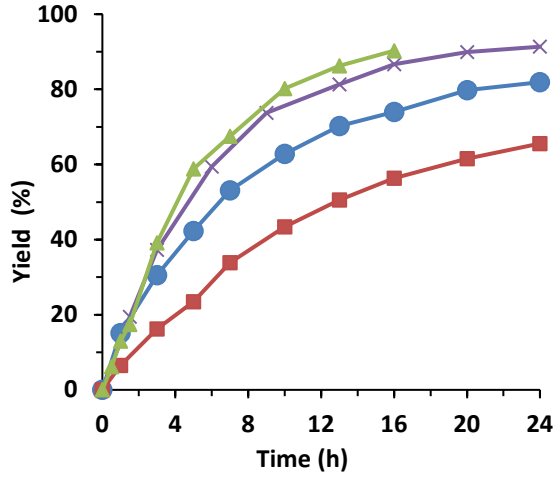

Figure 6. The yield of different esters were plotted versus time when esterification was performed in the presence of Al-ITQ-SO_3H: ethyl hexanoate (×) using 10 mol% SO_3H at 90ºC and ethanol as solvent<; (●) butyl hexanoate using 10 mol% SO_3H at 90ºC and butanol as solvent; (■) hexyl hexanoate using 10 mol% SO_3H at 90ºC and hexanol as solvent; (▲) hexyl hexanoate using 10 mol% SO_3H at 120ºC and hexanol as solvent.

The catalytic performance of Al-ITQ-SO_3H for the esterification reaction of hexanoic acid with methanol, at 60ºC, was firstly checked (Scheme 3). Figure S11 illustrated the high catalytic activity exhibited for the hybrid catalyst achieving 95% of yield at short reaction time by using 10 mol% SO_3H as catalyst loading. In order to ensure that not any active substance migrates from the Al-ITQ-SO_3H material to the liquid phase and could be responsible, at least in part, of the catalytic performance, a leaching test was performed. After 3 hours of reaction time, the Al-ITQ-SO_3H catalyst was removed by filtration and the process was continued. After that, the reaction was continued and samples were taken until 20 hours

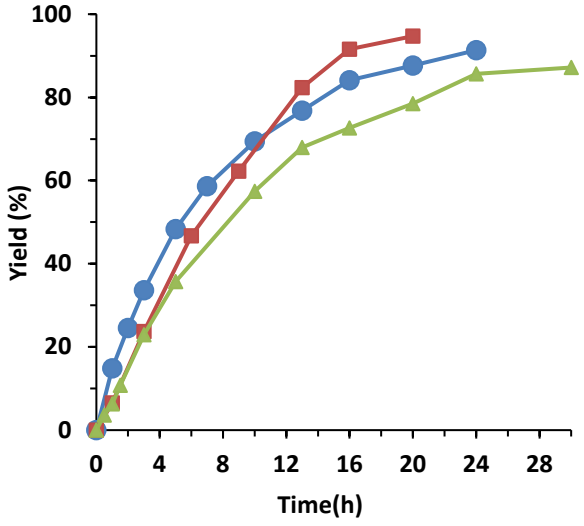

Figure 7. The yield of different esters were plotted versus time when esterification was performed in the presence of Al-ITQ-SO_3H: (■) methyl hexanoate, (●) methyl octanate and (▲) methyl laurate. Reaction conditions: 10 mol% SO_3H at 60ºC, using methanol as solvent.

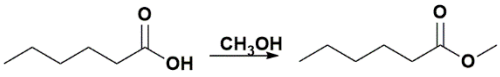

Scheme 3. Formation of methyl hexanoate.

of reaction time. Figure S11 showed that the yield did not suffered substantially changes. Taking into account the high methyl hexanoate yield obtained and the stability of Al-ITQ-SO_3H as acid catalyst, the preparation of esters with applications as flavours agents for their fruity and sweetly odour and pineapple nuance, using alcohols with different chain lengths such as ethanol, butanol and hexanol was carried out. The yield of each ester versus time was plotted in the Figure 6. When alcohols with higher chain length were used, such as butanol and hexanol, the yield decreased from 91 to 65%. An increase of the number of carbon atoms in the alcohol chain produces an inductive effect contributing to increase the nucleophilic reactivity of the alcohol group. Therefore, the observed decrease of yield was attributed to steric effect and adsorption/desorption limitations that can be improved with an increase of temperature. Therefore, it was possible to achieve a 90% hexyl hexanoate yield when the temperature was increased until 120ºC, after 16h of reaction time.

Additionally, methyl esters of octanoic and lauric were prepared. Both esters find application as flavours and fragrances agents due to their green fruity and citrus odour and, soapy, creamy and coconut odour, respectively. Different factors can influence the carboxylic acid reactivity. Indeed, an increase of alkyl chain length of the acid produces an inductive effect contributing to decrease the electrophilic reactivity of the acid group. Moreover, steric effect and adsorption/desorption limitations are expected. Nonetheless, 91% methyl octanoate yield after 24 h of reaction and 87% methyl laurate yield after 30 h, at 60ºC were achieved. The Figure 7 illustrated that initial rate of reaction decreased when the acid chain length increased as it could be expected, achieving very good esters yield.

These results evidenced the excellent catalytic performance exhibited by Al-ITQ-SO_3H material to produce esters with different characteristics and industrial interest in flavours and fragrances industry.

Open ring reactions

Epoxides are important synthetic intermediates in organic synthesis and in pharmaceuticals fine chemicals and also biological active compounds.[66-69] One of the most relevant transformations of epoxides is the ring opening to produce a broad range of bi-functional products depending of the nature

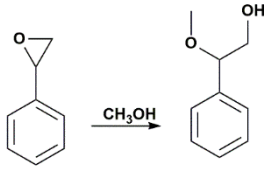

Scheme 4. Formation of 2-metoxy-2-phenylethanol.

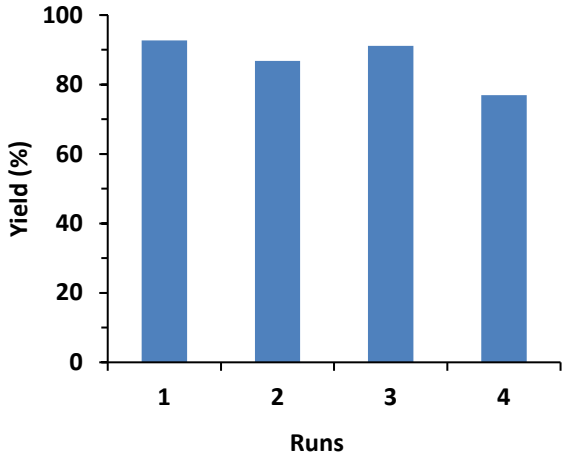

Figure 8. Al-ITQ-SO_3H catalyst was used for four consecutive uses for benzaldehyde dimethyl acetal production. Reaction conditions: 5 mol% SO_3H as catalyst, methanol as solvent, 30ºC, N_2 atmosphere. Reaction time: 7 h for the first use, 10h for the second and third use , and 15 h for the forth use.

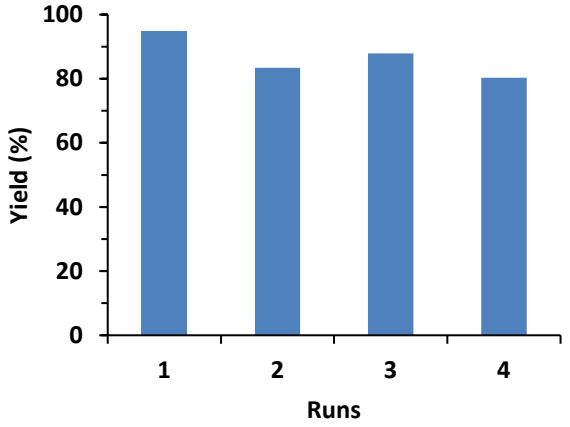

Figure 9. Al-ITQ-SO_3H catalyst was used for four consecutive uses for methyl hexanoate production. Reaction conditions: 10 mol% SO_3H, methanol as solvent, 60ºC. Reaction time: 20 h for the first, 24 h for second use and 30 h for the third use and 48 h for the forth use.

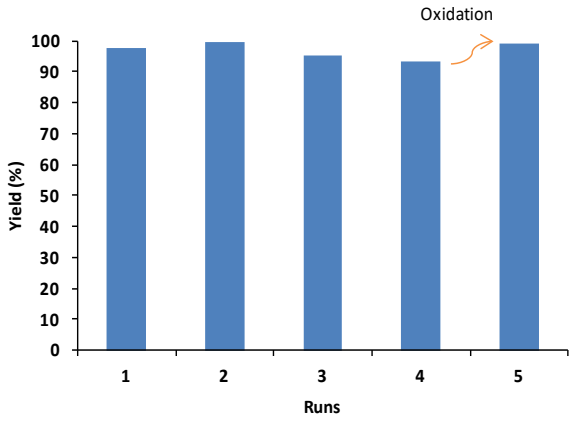

Figure 10. Al-ITQ-SO_3H catalyst was used for five consecutive uses for 2-metoxy-2-phenylethanol production. Reaction conditions: 10 mol% SO_3H, methanol as solvent, 30ºC. Reaction time: 3 h for the first, second and third use, 18 h for forth use and 3h for the fifth use.

of the nucleophile reactant thanks to the electrophilic character of the heterocyclic moiety and the ring strain. Particularly, alcohols allow to produce β-alkoxyalcohols catalysed by acids or bases to produce β-alkoxyalcohols with application in pharmaceuticals and solvent industry. Ring-opening reactions can proceed by either SN2 or SN1 mechanisms and is determined by the structural features of the epoxides and the reaction conditions. Generally, basic conditions involves SN2 mechanism while acid conditions proceeds via SN1 mechanism. This process has been deeply studied through different catalytic systems, using conventional homogenous catalysts and also heterogeneous catalysts such as amberlyst-15, clays, zeolites, MOFs.[70-73] Nevertheless, the development of new materials that allow reaching high yields and regio-selectivity under mild and green conditions are always a challenge. Likewise, considering the high catalytic properties as Brønsted acid sites of sulfonic groups of the Al-ITQ-SO_3H material, its catalytic behaviour for open ring reaction of styrene oxide with methanol was studied (Scheme 4). The catalyst loading was evaluated with testing three different charge of acid sites, i. e. 5, 7.5 and 10 mol% SO_3H. Figure S12 demonstrated that full conversion was reached after few hours of reaction time and that initial rate was similar for the three charges of catalyst. In comparison with results reported in the bibliography, higher and similar catalytic activity than copper or iron metal-organic materials were achieved (Table S3).

Study of stability and recyclability

The stability of catalytic properties and structure of Al-ITQ-SO_3H material under reactions conditions of three different processes presented above was studied. In order to be sure that no active species migrate from the solid to the liquid phase and could be responsible, at least in part, of the catalytic activity, a leaching test filtering off the solid catalyst at 25-50 % of yield was performed. Figures S11, S13 and S14 illustrated how the yield remained constant until the end of reaction, ensuring that no active species migrated from the catalyst to the reaction medium and were responsible of the monitored catalytic performance. Moreover, the reactions were also carried out with Al-ITQ-SH and MIL-53(Al) materials as solid catalysts, achieving low yields (Figure S13, Tables S2 and S3), confirming that the aluminum nodes present in the 1D sub-units were not able to perform the acetalization, ring opening or esterification, since Al-ITQ-SH and MIL-53(Al) catalysts exhibited practically no activity under the reaction conditions. Furthermore, these results evidenced that thiol groups did not present adequate catalytic properties to carry out the different studied processes, confirming the successful oxidation process to convert inactive thiol groups into active sulfonic acid sites. The spacer used in the assembly of the aluminum metal-organic hybrid materials (4-mercaptobenzoic acid) was also tested and exhibited lower activity than Al-ITQ-SO_3H material. Finally, the recyclability and reusability of the catalyst was examined, being the hybrid catalysts successfully reused for four consecutive runs for the three type of studied reactions (Figures 8, 9 and 10). The catalysts was recovered at the end of the reaction by filtration, washed with methanol, dried and reused. High catalytic activity

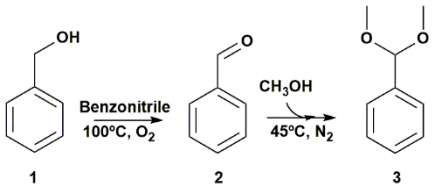

Scheme 5. One-pot consecutive oxidation-acetalization reaction.

was registered for all the studied processes, with a slight decrease for the last use, specifically for acetalization and esterification from 92 to 76% and 94 to 80%, respectively. Figures S15, S16 and S17 present the XRD patterns of the solids catalysts for all uses, being corroborated the high stability of the Al-ITQ-SO_3H structure under the reaction conditions during consecutives cycles. Because a slight loss of activity was noted for acetalization and esterification, the recycling study was repeated submitting the catalyst to an oxidation treatment after each use. In this way, we hope to ensure the oxidation of residual thiol group, the regeneration of the sulfonic groups and a deep cleaning of the catalytic surface. Figures S18, S19, S20 and S21 confirmed the effectiveness of the oxidation treatment to guarantee the catalytic performance the hybrid material along its recycles for the different reaction processes, being conserved the lamellar structure and crystallinity of the hybrid catalysts as it is observed from XRD patterns of the metal-organic catalyst after each catalytic cycles.

In summary, metal-organic materials with highly active sulfonic groups were prepared and used in acid catalysed reactions under mild conditions, showing high stability and reusability.

Oxidation-Acetalization one-pot two-step reaction

Up to now, the direct synthesis of acetals from alcohols have not been extensively reported, being a great challenge to perform consecutive two-step processes in one-pot reaction. Indeed, cascade and consecutive one-pot reactions present several advantages, such as avoiding separation and purification steps, saving energetic costs and generating environmentally more sustainable processes.[34] Specifically, described catalysts used for carrying out alcohol oxidation and acetalization reactions were meanly Pd-mineral acids, magnesium oxide, Pd-metalloporphyrin or Pd-UiO66-NH_2.[74-77] As valuable alternative, a specific bi-functional metal-organic catalyst combining Brønsted acid and redox active sites, Al-ITQ-SO_3H/Pd was prepared. The studied two steps reaction consists in the first step in the oxidation of benzyl alcohol (1) into benzaldehyde (2) under O_2 atmosphere catalysed by Pd nanoparticles, and in the second step in the acetalization of benzaldehyde with methanol to give the corresponding dimethylacetal (3) (Scheme 5). At first, the influence of the charge of Al-ITQ-SO_3H/Pd catalyst was studied using 1, 3 and 5

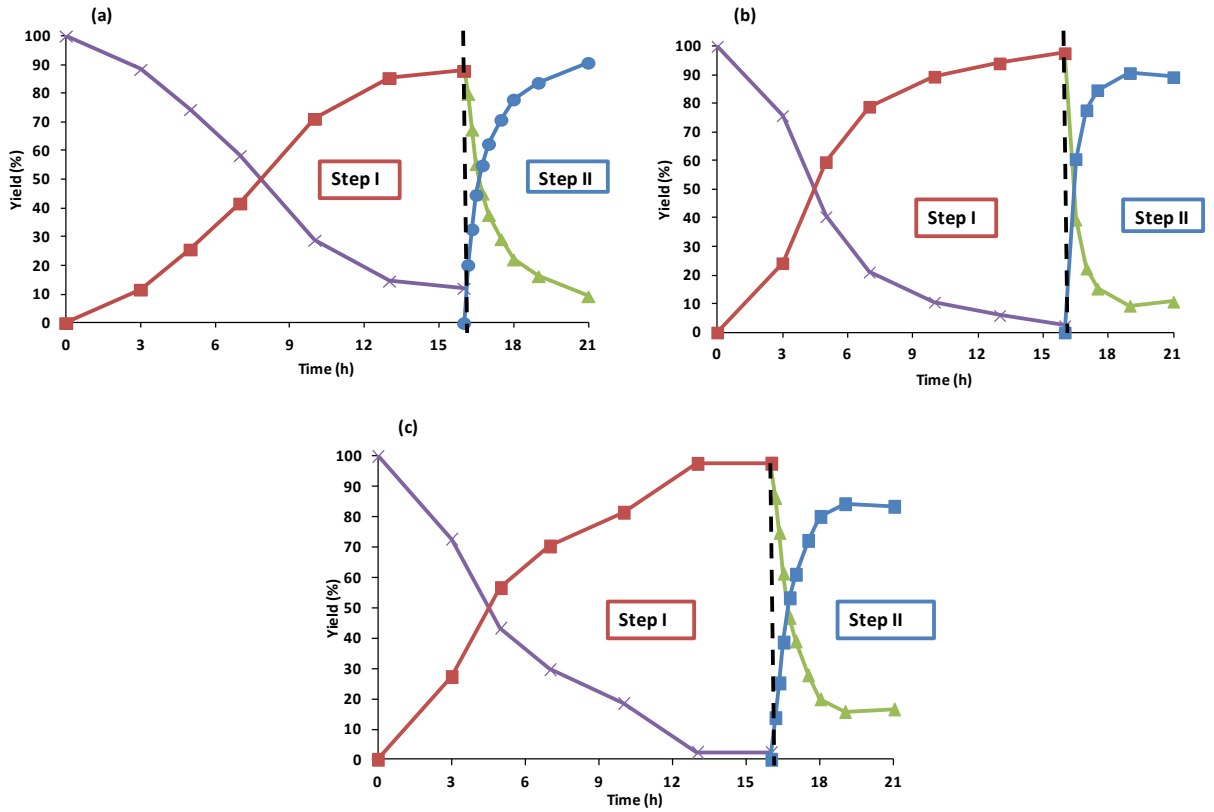

Figure 11. Kinetics of oxidation-acetalization reaction in presence of Al-ITQ-SO_3H/Pd catalyst with different loading of active sites: (a) 1 mol% Pd, (b) 3 mol% Pd and (c) 5 mol% Pd. (x) benzyl alcohol converted and (■) benzaldehyde produced in the step I using benzonitrile as solvent at 100ºC under O_2 atmosphere. (▲) benzaldehyde converted and (●) benzaldehyde dimethyl acetal produced in the step II using methanol as solvent at 45ºC under N_2 atmosphere.

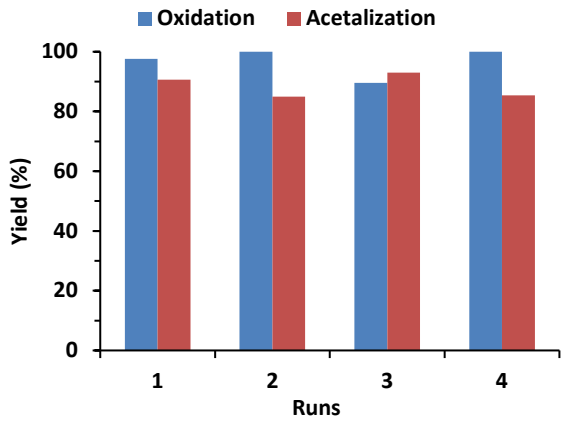

Figure 12. Four consecutive uses were represented for oxidation-acetalization process in presence of Al-ITQ-SO_3H/Pd with 3 mol% Pd used as catalyst.

mol% Pd to perform the consecutive reactions. Figure 11 showed that yield in the first step increased with an increase of Pd mol% from 87 % up to 97 %. Nevertheless, the yield in the second step decreased until 80% with an increase of Pd mol%. Then, a compromise between the Pd mol% and the maximum yield of each stage was found for a 3 mol% Pd, achieving a 97% yield in the first step and 90% yield in the second step. In comparison with literature, the catalytic performance of the Al-ITQ-SO_3H/Pd were higher than Pd@Cu-MOFs and similar to Pd@UiO67 and Pd@MIL-101.[78-81] Finally, the stability of the Al-ITQ-SO_3H/Pd was explored under the reaction conditions of consecutive oxidation-acetalization processes. A leaching test was performed filtering off the solid catalyst after 5 h of reaction time (59%). From Figure S22 it can be seen that no change in the yield until the end of reaction was observed. This result made sure of the absence of active palladium species in the reaction medium and, supported the heterogeneity of the process. Furthermore, additional experiments showed that the reaction did not take place when Al-ITQ-SO_3H, Al-ITQ-SH and MIL-53(Al) materials (without Pd redox active sites) were used as catalyst (Table S4), and neither in the presence of palladium precursor, reaching low yield at the same reaction time and conditions, showing the importance to combine both actives sites to carry out the one-pot two-step reaction process. This confirms unambiguously that the contribution of Pd nanoparticles located in the metalorganic architecture was necessary to perform the tandem catalytic reaction.

Additionally, recyclability and reusability of the bi-functional metal-organic material was checked. The Al-ITQ-SO_3H/Pd was active in the consecutive oxidation-acetalization reactions for four consecutive runs (Figure 12). After each run, the catalyst was filtered, washed with methanol, dried and reused. XRD patterns of the Al-ITQ-SO_3H/Pd material after each catalytic cycle was depicted in Figure S23. The lamellar structure is preserved along the different recycle while a slight crystallinity loss can be detected. Moreover, after the consecutive oxidation-acetalization consecutive runs, the recovered Al-ITQ-SO_3H/Pd hybrid catalyst contained similar Al and Pd content that fresh catalyst (Table 1), confirming that the composition and integrity of the bi-functional hybrid material were preserved during the successive catalytic cycles.

These results confirmed that a new bi-functional hybrid metal-organic material was synthesized, exhibiting high catalytic activity in one-pot two-step oxidation-acetalization reactions and high stability since its activity was maintained for four successive runs. Herein, we reported the synthesis of a new and promising redox-acid catalyst to perform consecutive and cascade processes.

Experimental

Chemicals

Hybrid metal-organic materials were synthesized by using 4-mercaptobenzoic acid (-SH, Aldrich) as organic source. Aluminum nitrate nonahydrate ($Al(NO_3)_3.9H_2O$, Aldrich) was used as inorganic source. Mixtures of dimethylformamide (DMF, Across) and MilliQ water were used as solvents in the solvothermal synthesis process. Bis(benzonitrile)palladium (II) chloride was used as precursor of palladium nanoparticles and methanol was used to remove linkers excess and to exchange solvent molecules occluded during the synthesis process. Moreover, hydrogen peroxide (30 %wt) was used to oxidize thiols to sulfonic pending groups.

Al-ITQ-SH

This organic-inorganic material was synthesized dissolving the organic spacer (-SH, 5.33 mmol) in a DMF/MilliQ water mixture (20 and 25 mL, respectively) at 90ºC. After that, the inorganic source ($Al(NO_3)_3.9H_2O$, 5.33 mmol) was easily dissolved in water (5mL) at room temperature. Both solution were mixed and kept under refluxed at 90ºC during 5 days. The precipitated powder was isolated by filtration with DMF and distilled water. Then, the solid obtained was washed several times with methanol and dried overnight at 100ºC under vacuum.

Al-ITQ-SH/Pd

The hybrid material with palladium nanoparticles was obtained in one-pot step synthesis, following the same procedure described for Al-ITQ-SH, but adding the palladium precursor (Bis(benzonitrile)palladium (II)) when the organic spacer was completely dissolved. After, the inorganic source was introduced and a clear solution was obtained, being kept it for 5 days. It was used the same method above describe to isolate the final material.

Al-ITQ-SO_3H and Al-ITQ-SO_3H /Pd

The materials above described were treated under an oxidation process in order to convert thiols in sulfonic moieties. Each material (300 mg) was introduced into a flask bottle with a 1M solution of hydrogen peroxide (15 mL) in ethanol at 90ºC for 24 h. After of this treatment, the solids were recovered by filtration with abundant ethanol in order to remove the guest molecules of hydrogen peroxide solution and the organic linker located

out of the framework. Finally, the solids were dried at 100ºC under vacuum.

MIL-53(Al)

Conventional 3D MIL-53(Al) was synthesized using 1,4-benzenedicarboxylic acid as organic linker (BDC, Aldrich), according to a literature procedure.[82]

Acetalization reactions

Formation of benzaldehyde dimethyl acetal
2 mL conic vessel was charged with different amount of catalyst (5, 7.5 or 10 mol% SO_3H) in 1 mL of methanol. Finally, benzaldehyde (0.33 mmol) was introduced and the reaction mixture was stirred for the required time at 30ºC under N_2 atmosphere.
Formation of benzaldehyde and vanillin propylene glycol acetal Reaction was tested in a three-necked round-bottom flask connected with a reflux condenser and with a Dean-Stark trap. Adequate amount of catalyst (10-20 mol% SO_3H) and 1,2-propanediol (ratio benzaldehyde:diol, 1:2 or 1:6) were added in 10 mL of toluene. After this, benzaldehyde or vanillin (3.3 mmol) was introduced and adequate reaction temperature was achieved (90-150 ºC) with vigorous stirring under N_2 atmosphere.

Esterification of aliphatic acids

Esterification reaction of aliphatic acids was carried out in a 2 mL conic vessel. The procedure consisted in charging the reactor with the adequate amount of catalyst (10 mol% SO_3H) and with 1 mL of alcohol. Then, aliphatic acid (0.4 mmol) was added and selected temperature was achieved (60-90ºC) under vigorous stirring.

Open ring reaction

Ring-opening reaction was carried out in a 2 mL conic vessel that was charged with different loading of catalyst (5, 7.5 or 10 mol% SO_3H) in 1 mL of methanol. After this, styrene oxide (0.25 mmol) was added and the reaction mixture was stirred at 30ºC for the required time.

Oxidation-Acetalization reaction

The reaction was carried out in one-pot two-step process using the bi-functional hybrid catalyst that contains palladium nanoparticles in the framework (Al-ITQ-SO_3H/Pd). First, 2 mL conic vessel was charged with different amount of active sites (1, 3 or 5 mol% Pd) in 1 mL of benzonitrile and benzyl alcohol (0.2 mmol) was introduced, being fixed the adequate temperature (100ºC) to carry out the first step, with vigorous stirring under oxygen atmosphere. After that the first step was completed, 1 mL of methanol was introduced and the temperature maintained at 45ºC under nitrogen atmosphere with continuous stirring.

Conclusions

A new low-dimensional family of aluminum metal-organic materials with thiol moieties were directly obtained through solvothermal synthesis routes. Characterization by XRD, chemical analysis, TGA, NMR, IR and XPS spectroscopy, and TEM/HRTEM microscopy corroborated the lamellar structure present in the framework of the hybrid materials based on the association of 1D organic-inorganic nanoribbon-type sub-domains. The accessible thiol groups were effectively transformed in free sulfonic pendant centres by oxidation treatment, being the hybrid materials successfully tested in several acid reactions, such as acetalization, esterification and open ring of epoxides with large scope in fine chemistry processes. The catalytic results confirmed the high catalytic activity of the lamellar metalorganic hybrid materials and their reusability and recyclability. Furthermore, bi-functional hybrid catalysts were synthesized in one-step direct solvothermal synthesis process, containing sulfonic pendant groups and Pd nanoparticles cohabitating in the structure, which were effective to carry out one-pot two-step oxidation-acetalization reactions, reaching high yield and activity during four consecutive uses. Definitively, a new and promising redox-acid low-dimensional MOF-type catalyst capable to perform consecutive and cascade processes was described, using monotopic functional organic spacers together with stabilized metallic nanoparticles, opening the possibilities to generate further heterogeneous multi-functional hybrid catalysts.

Conflicts of interest

There are no conflicts to declare.

Acknowledgements

The authors are grateful for financial support from Spanish Government, MAT2017-82288-C2-1-P and Severo Ochoa Excellence Program SEV-2016-0683, and MULTY2HYCAT (EU-Horizon 2020 funded project under grant agreement no. 720783).

Notes and references

1. T. Asefa, M. J. MacLachlan, N. Coombs and G. A. Ozin, G. A., *Nature,* 1999**, 402**, 867.
2. U. Díaz and A. Corma, A., *Coord. Chem. Rev.,* 2016**, 311**, 85.
3. S. Seth and A. J. Matzger, A. J., *Crys. Growth Des.,* 2017**, 17**, 4043.
4. D. J. Tranchemontagne, J. L. Mendoza-Cortes, M. O'Keeffe and O. M. Yaghi, *Chem. Soc. Rev.,* 2009**, 38**, 1257.
5. M. O'Keeffe and O. M. Yaghi, *Chem. Rev.,* 2012**, 112**, 675.
6. S. L. James, *Chem. Soc. Rev.,* 2003**, 32,** 276.
7. A. H. Chughtai, N. Ahmad, H. A. Younus, A. Laypkov and F. Verpoort, *Chem. Soc. Rev.,* 2015**, 44**, 6804.
8. S. M. J. Rogge, A. Bavykina, J. Hajek, H. Garcia, A. I. Olivos-Suarez, A. Sepulveda-Escribano, A. Vimont, G. Clet, P. Bazin, F. Kapteijn, M. Daturi, E. V. Ramos-Fernandez, F. X. Llabres i Xamena, V. Van Speybroeck and J. Gascon, *Chem. Soc. Rev.,* 2017**, 46**, 3134.
9. J. -R. Li, R. J. Kuppler and H. -C Zhou, *Chem. Soc. Rev.,* 2009**, 38**, 1477.

10. F. -Y. Yi, D. Chen, M. -K. Wu, L. Han and H. -L. Jiang, H.-L., *ChemPlusChem,* 2016**, 81**, 675.
11. C. -Y. Sun, C. Qin, X. -L. Wang and Z. -M. Su, *Expert Opinion on Drug Delivery,* 2013**, 10**, 89.
12. V. Stavila, A. A. Talin and M. D. Allendorf, *Chem. Soc. Rev.,* 2014**, 43**, 5994.
13. J. Lee, O. K. Farha, J. Roberts, K. A. Scheidt, S. T. Nguyen, J. T. Hupp, *Chem. Soc. Rev.,* 2009**, 38**, 1450.
14. A. Corma, H. Garcia and F. X. Llabres i Xamena, *Chem. Rev.,* 2010**, 110**, 4606.
15. P. Garcia-Garcia, M. Muller and A. Corma, *Chem. Sci.,* 2014**,** *5*, 2979.
16. O. K. Farha, A. M. Shultz, A. A. Sarjeant, S. T. Nguyen and J. T. Hupp, *J. Am. Chem. Soc.,* 2011**, 133**, 5652.
17. C. Zou, Z. Zhang, X. Xu, Q. Gong, J. Li and C. -D. Wu, *J. Am. Chem. Soc.,* 2012**, 134**, 87.
18. P. W. Siu, Z. J. Brown, O. K. Farha, J. T. Hupp and K. A. Scheidt, *Chem. Commun.,* 2013**, 49**, 10920.
19. M. Hartmann and M. Fischer, *Microporous Mesoporous Mater.,* 2012**, 164**, 38.
20. Z. Hasan, J. W. Jun and S. H. Jhung, *Chem. Eng. J.,* 2015**, 278**, 265.
21. J. Jiang and O. M. Yaghi, *Chem. Rev.,* 2015**, 115**, 6966.
22. M. G. Goesten, J. Juan-Alcañiz, E. V. Ramos-Fernandez, K. B. Sai Sankar Gupta, E. Stavitski, H. van Bekkum, J. Gascon and F. Kapteijn, *J. Catal.,* 2011**, 281,** 177.
23. D. Britt, C. Lee, F. J. Uribe-Romo, H. Furukawa and O. M. Yaghi, *Inorg. Chem.,* 2010**, 49**, 6387.
24. J. Juan-Alcaniz, J. Gascon and F. Kapteijn, *J. Mater. Chem.,* 2012**,** *22* , 10102.
25. G. Akiyama, R. Matsuda, H. Sato, M. Takata and S. Kitagawa, *Adv. Mater.,* 2011**, 23**, 3294.
26. M. Lin Foo, S. Horike, T. Fukushima, Y. Hijikata, Y. Kubota, M. Takata and S. Kitagawa, *Dalton Trans.,* 2012**, 41**, 13791.
27. S. Biswas, J. Zhang, Z. Li, Y. -Y. Liu, M. Grzywa, L. Sun, D. Volkmer and P. Van Der Voort, *Dalton Trans.* 2013**, 42**, 4730.
28. Y. Zang, J. Shi, F. Zhang, Y. Zhong and W. Zhu, *Catal. Sci. Technol.,* 2013**, 3**, 2044.
29. J. Jiang, F. Gándara, Y. -B. Zhang, K. Na, O. M. Yaghi and W. G. Klemperer, *J. Am. Chem. Soc.,* 2014**, 136**, 12844.
30. Y. Jin, J. Shi, F. Zhang, Y. Zhong and W. Zhu, *J. Mol. Catal A Chem.,* 2014**, 383-384**, 167.
31. J. Chen, K. Li, L. Chen, R. Liu, X. Huang and D. Ye, *Green Chem.,* 2014**, 16**, 2490.
32. D. E. Fogg and E. N. dos Santos, *Coord. Chem. Rev.,* 2004**, 248**, 2365.
33. P. T. Anastas, *Chem. Rev.,* 2007**, 107**, 2167.
34. M. J. Climent, A. Corma, S. Iborra and M. J. Sabater, *ACS Catal.,* 2014**, 4**, 870.
35. D. Zhao, D. J. Timmons, D. Yuan and H. -C. Zhou, *Acc. Chem. Res.,* 2011**, 44**, 123.
36. F. G. Cirujano, F. X. Llabres i Xamena and A. Corma, *Dalton Trans.,* 2012**, 41**, 4249.
37. F. G. Cirujano, A. Leyva-Pérez, A. Corma and F. X. Llabrés i Xamena, *ChemCatChem,* 2013**, 5**, 538.
38. R. Srirambalaji, S. Hong, R. Natarajan, M. Yoon, R. Hota, Y. Kim, Y. Ho Ko and K. Kim, *Chem. Commun.,* 2012**, 48**, 11650.
39. A. Dhakshinamoorthy and H. Garcia, *ChemSusChem,* 2014**, *7*,** 2392.
40. H. -L. Jiang and Q. Xu, *Chem. Commun.,* 2011**, 47**, 3351.
41. F. Wu, L. -G. Qiu, F. Ke and X. Jiang, *Inorg. Chem. Commun.,* 2013**, 32**, 5.
42. M. Sabo, A. Henschel, H. Frode, E. Klemm and S. Kaskel, *J. Mater. Chem.,* 2007**, 17**, 3827.
43. T. Ishida, M. Nagaoka, T. Akita and M. Haruta, *Chem. Eur. J.,* 2008**, 14**, 8456.
44. A. Aijaz, A. Karkamkar, Y. J. Choi, N. Tsumori, E. Rönnebro, T. Autrey, H. Shioyama and Q. Xu, *J. Am. Chem. Soc.,* 2012**, 134**, 13926.
45. H. -L. Jiang, B. Liu, T. Akita, M. Haruta, H. Sakurai and Q. Xu, *J. Am. Chem. Soc.,* 2009**, 131**, 11302.
46. P. Fiurasek and L. Reven, *Langmuir*, 2007, **23**, 2857-2866.
47. W. E. Moddeman, W. C. Bowling, D. C. Carter and D. R. Grove, *Surf. Interface Anal.,* 1988**, 11**, 317.
48. P. W. Ju, J. Hyuna, L. W. Ram, S. J. Hwa, Y. Kicheon, K. BongSoo and H. C. Seop, *Angew. Chem. Int. Ed.,* 2015**, 54**, 5142.
49. M. A. Avery, *J. Med. Chem.,* 1999**, 42**, 5285.
50. M. J. Ashton, C. Lawrence, J. -A. Karlsson, K. A. J. Stuttle, C. G. Newton, B. Y. J. Vacher, S. Webber and M. J. Withnall, *J. Med. Chem.,* 1996**, 39**, 4888.
51. H. Surburg and J. Panten, Individual Fragrance and Flavor Materials. In *Common Fragrance and Flavor Materials*, Wiley-VCH Verlag GmbH & Co., **2006**, 7-175.
52. E. Wenkert and T. E. Goodwin, *Synth. Commun.,* 1977**, 7**, 409.
53. T. -J.Lu, J. -F. Yang, L. -J. Sheu, *J. Org. Chem.,* 1995**, 60**, 2931.
54. M. N. Timofeeva, V. N. Panchenko, J. W. Jun, Z. Hasan, M. M. Matrosova and S. H. Jhung, *Appl. Catal. A Gen.,* 2014**, 471**, 91.
55. A. Corma, M. J. Climent, H. García and J. Primo, *Appl. Catal.,* 1990**, 59**, 333.
56. V. R. Ruiz, A. Velty, L. L. Santos, A. Leyva-Pérez, M. J. Sabater, S. Iborra and A. Corma, *J. Catal.,* 2010**, 271**, 351.
57. T. Kawabata, T. Mizugaki, K. Ebitani and K. Kaneda, *Tetrahedron Lett.,* 2001**, 42**, 8329.
58. M. J. Climent, A. Corma, S. Iborra, M. C. Navarro and J. Primo, *J. Catal.,* 1996**, 161**, 783.
59. Esterification: Methods, Reactions and Applications By J. Otera. Wiley VCH, Weinheim, **2003**, 303 pp.
60. N. C. Deno, *J. Chem. Educ.,* 1971**, 48**, A218.
61. J. Gimenez, J. Costa and S. Cervera, *Ind. Eng. Chem. Res.* 1987**, 26**, 198.
62. T. J. Schildhauer, I. Hoek, F. Kapteijn and J. A. Moulijn, *Appl. Catal. A Gen.,* 2009**, 358**, 141.
63. A. Alsalme, E. F. Kozhevnikova and I. V. Kozhevnikov, *Appl. Catal. A Gen.,* 2008**, 349**, 170.
64. B. R. Jermy and A. Pandurangan, *Appl. Catal. A Gen.,* 2005**, 288**, 25.
65. G. D. Yadav and M. B. Thathagar, *React. Funct. Polym.,* 2002**, 52**, 99.
66. R. S. Coleman, *J. of Med. Chem.,* 1996**, 39**, 1010.
67. I. Vilotijevic and T. F. Jamison, *Angew. Chem. Int. Ed.,* 2009**, 48**, 5250.
68. J. Gorzynski Smith, *Synthesis,* 1984**, 8**, 629.
69. E. J. Corey, S. Shibata and R. K. Bakshi, *J. Org. Chem.,* 1988**, 53**, 2861.
70. Y. -H. Liu, Q. -S. Liu and Z. -H. Zhang, *J. Mol. Catal. A Chem.,* 2008**, 296**, 42.
71. M. Guidotti, R. Psaro,N. Ravasio, M. Sgobba, F. Carniato, C. Bisio, G. Gatti and L. Marchese, *Green Chem.,* 2009**, 11**, 1173.
72. O. Makoto, K. Motomitsu and I. Yusuke, *Chem. Lett.,* 1985**, 14**, 779.
73. A. Dhakshinamoorthy, M. Alvaro and H. Garcia, *Chem. Eur. J.* 2010**, 16**, 8530.
74. A. C. Bueno, J. A. Gonçalves and E. V. Gusevskaya, *Appl. Catal. A Gen.,* 2007**, 329**, 1.

75. M. I. Vohra, D. -J. Li, Z. -G. Gu and J. Zhang, *Nanoscale,* 2017**, 9**, 7734.
76. B. M. Smith and A. E. Graham, *Tetrahedron Lett.,* 2007**, 48**, 4891.
77. X. Li, Z. Guo, C. Xiao, T. W. Goh, D. Tesfagaber and W. Huang, *ACS Catal.,* 2014**, 4**, 3490.
78. P. García-García, M. Müller and A. Corma, *Chem. Sci.,* 2014**, 5**, 2979.
79. L. Y. Chen, H. Chen, R. Luque and Y. W Li, *Chem. Sci.,* 2014**, 5**, 3708.
80. G. Chen, S. Wu, H. Liu, H. Jiang and Y. Li, *Green Chem.,* 2013**, 15**, 230.
81. G. -J. Chen, J. -S. Wang, F. -Z. Jin, M. -Y. Liu, C. -W. Zhao, Y. -A. Li and Y. -B. Dong, *Inorg. Chem.,* 2016**, 55**, 3058.
82. G. Cai and H.-L. Jiang, *Angew. Chem., Int. Ed*., 2017, **56**, 563–567.